THE EFFECT OF QUATERNARY ALLUVIUM ON STRONG GROUND MOTION IN THE COYOTE LAKE, CALIFORNIA, EARTHQUAKE OF 1979

by

William B. Joyner

Richard E. Warrick

Thomas E. Fumal

U.S. Geological Survey
Open-File Report 81-353

This report is preliminary and has not been reviewed for conformity with U.S. Geological Survey editorial standards and stratigraphic nomenclature.

ABSTRACT

The effect of alluvium on strong ground motion can be seen by comparing two strong-motion records of the Coyote Lake, California, earthquake of August 6, 1979 (M_L = 5.9). One record at a site on Franciscan bedrock had a peak horizontal acceleration of 0.13 g and a peak horizontal velocity of 10 cm/sec. The other, at a site 2 km distant on 180 m of Quaternary alluvium overlying Franciscan, had values of 0.26 g and 32 cm/sec, amplifications by factors of 2 and 3. Horizontal motions computed at the alluvial site for a linear plane-layered model based on measured P and S velocities show reasonably good agreement in shape with the observed motions but the observed peak amplitudes are greater by a factor of about 1.25 in acceleration and 1.8 in velocity. About 15 percent of the discrepancy in acceleration and 20 percent in velocity can be attributed to the difference in source distance; the remainder may represent focusing by refraction at a bedrock surface concave upward. There is no clear evidence of nonlinear soil response. Fourier spectral ratios between motions observed on bedrock and alluvium show good agreement with ratios predicted from the linear model. In particular, the observed frequency of the fundamental peak in the amplification spectrum agrees with the computed value, indicating that no significant nonlinearity occurs in the secant shear modulus. Computations show that nonlinear models are compatible with the data if values of the coefficient of dynamic shear strength in terms of vertical effective stress are in the range of 0.5 to 1.0 or greater. The data illustrate that site amplification may be less a matter of resonance involving reinforcing multiple reflections, and more the simple effect of the low near-surface velocity. Application of traditional seismological theory leads to the conclusion that the site amplification for

peak horizontal velocity is approximately proportional to the reciprocal of the square root of the product of density and shear-wave velocity.

INTRODUCTION

The Gilroy strong-motion array was established by the U.S. Geological Survey in 1970 to study the effect of local geology on strong ground motion in earthquakes. It is a linear array of six, three-component accelerographs extending 10 km from Franciscan rocks on the southwest across Quaternary alluvium of the Santa Clara valley to Cretaceous rocks of the Great Valley sequence on the northeast. The Coyote Lake earthquake occurred on the Calaveras fault near the northeast end of the array. Five records were obtained from the array including two of particular interest in studying the effect of geology on ground motion, the record from station 1 on Franciscan at the southwest end of the array and the record from station 2, two km to the northeast on 180 m of Quaternary alluvium overlying Franciscan (Figure 1). The effect of the alluvium was to amplify both horizontal and vertical motion. Peak horizontal acceleration at station 1 was 0.13 g and peak horizontal velocity 10 cm/sec. At station 2 values of 0.26 g and 32 cm/sec were recorded. At station 1 peak vertical acceleration was 0.08 g and peak vertical velocity 2.6 cm/sec versus 0.18 g and 6.6 cm/sec at station 2 (Porcella et al., 1979; Brady et al., 1980). These records provide an especially favorable opportunity to study the effect of sediments on earthquake ground motion at moderate amplitude levels.

Attempts to predict the response of soil to earthquake ground motion have a long history. An important pioneer was Kanai (1952) who solved the problem for a system of layers with linear viscoelasticity of the Voigt type excited by a vertically incident shear wave in the underlying elastic medium. Idriss and Seed (1968a, 1968b) warned against assuming linear soil behavior under conditions of strong ground motion. To deal with nonlinearity they introduced the "equivalent linear method", which is an iterative method based on the assumption that the response of the real soil can be approximated by the response of a linear model whose properties are chosen in accord with the average strain that occurs at each depth in the model during excitation. The strain-dependent soil properties are estimated on the basis of laboratory test data. More recently, a number of workers have described methods that use nonlinear stress-strain relationships directly (Streeter et al., 1974; Constantopoulos, 1973; Faccioli et al., 1973; Chen and Joyner, 1974). Joyner and Chen (1975) used a direct method to demonstrate that the equivalent linear method may significantly underestimate short period motions for thick soil columns and high levels of input motion.

The ground motion data available for testing these ideas has been meager. Such testing is desirable not only because of the simplifications necessarily introduced in devising mathematical models of site response, but also because of doubts about the degree to which laboratory measurements on soil are representative of the dynamic behavior of the soil in situ. Idriss and Seed (1968b) tried their method out on data from the 1957 San Francisco earthquake. These data were recorded on strong-motion accelerographs, but they have peak horizontal accelerations of 0.13 g or less and peak horizontal velocities of 5 cm/sec or less, too small to provide a decisive test of nonlinearity.

Borcherdt (1970, Borcherdt and Gibbs, 1976) made recordings in the San Francisco Bay area of distant nuclear explosions. These recordings showed marked variations in amplitude that were consistently related to the geology of the recording site. The indicated relationships between geology and ground-motion amplitude paralleled the relationship between geology and 1906 earthquake intensities as reported by Wood (1908) and Lawson (1908).

Ground motion data from downhole seismometer arrays have been considered by a number of authors. Data from an array at Tokyo Station were analyzed by Shima (1962) and Dobry et al., (1971); data from an array at Union Bay, Seattle by Seed and Idriss (1970), Tsai and Housner (1970), and Dobry et al. (1971); and data from an array near San Francisco Bay by Joyner et al. (1976). In all these cases general agreement was reported between the observations and the predictions of simple plane-layer theory, but in all the cases the motion was small in amplitude.

Rogers and Hays (1979; Hays et al., 1979) studied the consistency of site transfer functions between rock and soil sites for different events recorded at the same site. They concluded from the lack of dependence on amplitude that soil response remains linear up to rather high values of estimated strain, values up to 10^{-4} for data from the San Fernando earthquake and 10^{-3} for recordings of nearby nuclear explosions.

In this report we use data from the Coyote Lake earthquake to examine the effect of soil on strong ground motion with particular emphasis on the linearity of the response. We compare the observed data with the response computed for a plane-layered linear viscoelastic model and for plane-layered nonlinear models. We restrict our attention to the horizontal components of motion since they have the greater engineering importance.

THE EARTHQUAKE

The mainshock (M_L = 5.9) occurred on the Calaveras fault zone southeast of Coyote Lake near the town of Gilroy on August 6, 1979 (Lee et al., 1979, Uhrhammer, 1980). Focal depth was 9.6 km (± 2 km). Aftershock hypocenters for the first 15 days occurred along a 25 km segment of the fault lying principally to the southeast of Coyote Lake (Figure 1) with focal depths down to 12 km. Discontinuous surface faulting was observed along a 14.4 km length of the Calaveras fault southeast of Coyote Lake with a maximum offset of 5 mm near San Felipe Lake (Herd et al., 1979).

Although the aftershock zone extends about 20 km southeast of the mainshock hypocenter, it is not certain that the mainshock rupture extended that far. Archuleta (1979; personal communication, 1980) concluded from an analysis of the strong motion record at station number 6 of the Gilroy array that the rupture extended at least 8 km. Okubo (1979; personal communication, 1980) examined spectra of broad-band data recorded at Berkeley and concluded that the coherent rupture did not extend the full length of the aftershock zone.

The length of rupture affects the interpretation of the records at Gilroy stations number 1 and number 2 in the choice of an average azimuth for resolving the horizontal motion into radial and transverse components. On the basis of the available information, we choose (somewhat arbitrarily) a point 4 km southeast of the epicenter and determine the average azimuth from that point to stations 1 and 2. The result is S20°W.

SITE STUDIES

After the earthquake a systematic program of documenting site characteristics at the array sites was undertaken by J. F. Gibbs, T. E. Fumal, and R. M. Hazlewood. Holes were drilled, geologic logs prepared, and P and S velocity surveys carried out to a depth of 20 m at station 1, 30 m at stations 2, 4, and 6, and 60 m at station 3. Results of these studies are being prepared for separate publication. Since none of these first holes at the alluvial sites (stations 2, 3, and 4) penetrated the full thickness of alluvium, a second hole was drilled at station 2 to a depth of 197 m. Franciscan was encountered at the base of the alluvium at 180 m. A geologic log was made for the hole (Figure 2), and P and S velocity surveys were run. The velocity profiles are shown in Figure 3. We were unable to obtain reliable velocity measurements in the Franciscan bedrock at station 2; the values shown on Figure 3 and assumed in later calculations are obtained from the measurements in the shallow hole at station 1. The water table at station 2 is at a depth of 20 m, judging both by the standing water level in the well and by the results of the P velocity survey. A standard penetration test gave a count of 21 at a depth of 3 m at station 2.

Walter D. Mooney and others (unpublished data) have shot a refraction profile across the Santa Clara valley 2.7 km southeast of station 2. Preliminary interpretation (W. D. Mooney, personal communication, 1980) indicates that the Franciscan bedrock surface exposed southwest of the valley dips about 10 degrees to the northeast beneath the Quaternary alluvium of the valley. This agrees quite well with the 7 degree dip computed from the depth to Franciscan at station 2 and the distance to the edge of the alluvium. It is also consistent with the dip of approximately 14 degrees northeast that characterizes the exposed Franciscan surface southwest of the valley.

THE LINEAR MODEL

Kanai's (1952) original solution to the plane layer problem applied to the case of an SH wave vertically incident in a semi-infinite elastic medium overlain by three horizontal soil layers with viscoelasticity of the Voigt type. Matthiesen et al. (1964) adapted Kanai's solution to machine computation and extended it to an arbitrary number of layers. We use the same general approach extended to general viscoelastic behavior for the soil layers and extended with the aid of the matrix methods of Haskell (1953, 1960) to the case where the input wave in the underlying medium has arbitrary angle of incidence and to the case of incident SV as well as SH waves. Similar developments have been presented by Silva (1976) and A. F. Shakal (1979, Ph.D. thesis, Massachusetts Institute of Technology).

The viscoelastic properties of the soil layers were represented by using a complex shear modulus that can be written in real numbers as

$$\mu = \mu_R(1 + i/Q)$$

where the μ_R and Q are independent of frequency. Strictly speaking these assumptions lead to a violation of causality (Futterman, 1962), but in this case the transit time in the soil is so small that the effect should be negligible. Zero energy loss is assumed in compressional deformation and the bulk modulus is, accordingly, real.

Values for the moduli are determined from the measured P and S velocities and assumed densities of 2.0 gm/cm^3 for the soil and 2.6 gm/cm^3 for the rock. We do not have a measurement of Q at the site, and we assume a value of 16 based on measurements (Joyner et al., 1976) in similar materials in the San Francisco Bay area (equivalent to a damping ratio of about 3 percent). The velocity values used are shown in Figure 3.

To compute the angle of incidence at the base of the alluvium we first take the distance from the site to the reference point on the fault 4 km southeast of the epicenter and divide by the focal depth. This gives the tangent of the incidence angle at depth. Noting that the shear velocity at depth should be about 3 km/sec, whereas the shear velocity just below the alluvium is 2 km/sec, we apply Snell's law and obtain an incidence angle of 30° at the base of the alluvium. We assume that all of the incident motion is represented by S waves.

With these assumptions we use the Haskell methods to obtain the complex transfer functions between a site at the surface of the alluvium and a site with bedrock at the surface. The transfer functions are then used with the aid of the Fast Fourier Transform to obtain computed motions at the surface of the alluvium from the recorded motions at the site with bedrock at the surface. No allowance is made for the difference in source distance at the two sites. Results for the transverse component of motion are shown in Figure 4. The bottom trace is the observed acceleration at station number 1 on bedrock, the middle trace is the observed acceleration at station number 2 on the surface of the alluvium and the top trace is the acceleration computed for the surface of the alluvium using the plane-layered linear model. The computed trace is smaller in peak value than the observed trace, 0.17 g as opposed to 0.24 g, but there is good agreement in the wave form. As will be seen, some but not all of the amplitude difference can be explained by the difference in source distance. Similar results are shown for the radial component of acceleration on Figure 5, the transverse component of particle velocity on Figure 6 and the radial component of velocity on Figure 7.

In order to isolate the response characteristics of the site from the effects of the source we compute Fourier spectral ratios between the motion on alluvium and bedrock. The spectral ratios are computed in the following manner: The whole record is used. To avoid spectral leakage the accelerograms are first multiplied by a window that is flat in the central portion and has a cosine half-bell taper occupying 10 percent of the total window length at each end (Kanasewich, 1973, p. 93-94). The complex Fourier spectrum is then calculated using the Fast Fourier Transform and the square modulus of the spectrum is smoothed using a symmetrical 31 point triangular window. After smoothing, the square root is taken to give a smoothed modulus from which the ratios are computed. Use of a 31 point triangular window gives spectra with a resolution, after smoothing, of about 0.4 Hz. Theoretical spectral ratios are calculated using a method described by Joyner et al. (1976) to insure that the theoretical ratios show the same effects from windowing and smoothing as are present in the observed ratios. In addition to calculating spectral ratios from the whole records, we calculated ratios using a window, centered on the S wave, which was flat for 2.2 sec in the central portion and had a one-sec cosine half-bell taper at each end. The results did not differ significantly from the whole-record ratios and are not shown.

Comparisons of observed and theoretical spectral ratios are given in Figure 8 for the transverse and radial components. The observed ratios are consistently somewhat higher, but the agreement in shape is good. It is particularly important to note that there is no significant shift in frequency of the fundamental peak. This observation puts limits on the degree of nonlinearity that can be ascribed to the soil response.

NONLINEAR MODELS

We also do computations with nonlinear models to show that there is a range of properties for which nonlinear models are compatible with the data. We use the explicit method described by Joyner and Chen (1975) with one significant change, described below. The method is based on a rheological model proposed by Iwan (1967), which is illustrated in Figure 9. It is composed of simple linear springs and Coulomb friction elements arranged as shown. The friction elements remain locked until the stress on them exceeds the yield stress Y_i. Then they yield, and the stress across them during yielding is equal to the yield stress. By appropriate specification of the spring constants μ_i and the yield stresses Y_i we can model a very broad range of material behavior. There is one model of the kind diagrammed in Figure 9 for each soil layer in the system.

There is one problem with this model; the anelastic attenuation goes toward zero for small amplitude motion. As a result it may give good results for the high-level portion of a record but give excessive amplitudes in the low-level portion. We do not consider this a serious defect since it affects only the low-amplitude motion, but it is easy to remedy and we will do so. Problems like this are commonly solved by adding a dashpot to the system. We object to that approach because it produces an unrealistic dependence of damping coefficient upon frequency. What we do is replace the first linear spring μ_1 by a nonlinear spring of the appropriate kind. Such a nonlinear spring has been described by Andrews and Shlien (1972). When shear stress and shear strain rate have the same sign (loading) the spring is characterized by a constant modulus μ_0. When they have opposite sign the modulus is variable, given by

$$\mu = \mu_0 + \Delta\mu \ \frac{s}{s_{max}}$$

where s is the shear stress and s_{max} is the maximum shear stress reached in the previous loading cycle. The equivalent Q is controlled by the value of $\Delta\mu$. Straightforward integration give the relationship

$$\frac{1}{Q} = \frac{1}{\pi}\left[1 + 2\frac{\mu_o}{\Delta\mu}\left(\frac{\mu_o}{\Delta\mu}\log_e\left[1 + \frac{\Delta\mu}{\mu_o}\right] - 1\right)\right]$$

We use a value of 0.38 for ratio $\Delta\mu/\mu_o$, and this gives a low-strain Q of 16, the value assumed for the linear model.

The parameters of the model are chosen to give a hyperbolic stress-strain curve

$$e = \frac{s_\ell}{\mu}\frac{s}{s_\ell - s}$$

where e is shear strain and s_ℓ is the dynamic shear strength, the maximum shear stress the material can withstand. Values of μ and density for the soil layers are the same as used for the linear model. The maximum shear stress s_ℓ is assumed proportional to vertical effective stress P_{ve},

$$s_\ell = \gamma P_{ve}$$

and computations are performed for coefficients γ of 1.0 and 0.5. In computing vertical effective stress the water-table depth of 20 m is taken into account.

Results for the transverse component of acceleration are shown in Figure 10. The bottom trace is the observed acceleration at station number 1 on bedrock, the second trace is the observed acceleration at station number 2 on the surface of the alluvium, the third trace is the acceleration computed for the surface of the alluvium using the linear model, the fourth trace is computed using the nonlinear model with a coefficient of 1.0 for s_ℓ in terms of vertical effective stress, and the top trace is computed using the nonlinear model with a coefficient of 0.5. A similar comparison is shown in Figure 11 for the transverse component of velocity. The nonlinear models give somewhat smaller values of peak acceleration than the linear models but otherwise the results are very similar. A comparison of observed and computed peak acceleration and peak velocity values for all the models is given in Table 1. We may conclude that the nonlinear models are compatible with the data for values of the coefficient relating s_ℓ to vertical effective stress in the range of 0.5 to 1.0 or greater. It is necessary to emphasize, however, that these models are nonlinear only in the sense that they are capable of nonlinear behavior, not that they exhibit appreciable nonlinear behavior in this instance.

Peak strain was also computed for the nonlinear models. It was 3.3×10^{-4} achieved at a depth of about 110 m for both values of the coefficient. This is probably a good estimate of the strain that actually occurred, since the value is insensitive to the strength coefficient.

DISCUSSION

The results of calculations with linear models as shown in Figures 4 through 7 give waveforms in horizontal acceleration and velocity similar to the observed motion for both components. The peak observed motions are actually stronger than the computed motions in both components by a factor of about 1.25 in acceleration and 1.8 in velocity. Allowance for the difference in source distance using the attenuation curves of Boore et al. (1980) would reduce these values by 18 percent for acceleration and 25 percent for velocity. Using more recent curves (W. B. Joyner, D. M. Boore, and R. L. Porcella, manuscript in preparation), the reductions are 13 percent and 19 percent, respectively. We do not have enough information to give a unique explanation for the remaining discrepancy in amplitude, but if the bedrock surface beneath station 2 is concave upward, focusing could account for it (Boore et al., 1971; Hong and Helmberger, 1978). This explanation is given some support by the fact that the exposed Franciscan surface west of the edge of the alluvium projects to a greater depth at the site of station number 2 than the actual depth. This fact requires that there be concave curvature of the surface in the vicinity of station number 2.

The data show amplification on Quaternary alluvium in both acceleration and velocity and no clear evidence of nonlinearity. Significant nonlinearity in the secant shear modulus is precluded by the fact that the observed frequency of the fundamental response peak agrees with the frequency computed for a linear model. The data are compatible with nonlinear models in which the coefficient of dynamic shear strength in terms of vertical effective stress is in the range 0.5 to 1.0 or higher. Data at higher levels of motion will be required to demonstrate soil nonlinearity and to determine the threshold above which it occurs. The Coyote Lake data indicate that linear models are applicable to the response of soil to ground shaking at higher levels of motion than has been widely believed, levels of at least 0.25 g peak horizontal acceleration and 30 cm/sec peak horizontal velocity at the soil surface.

An important point concerning the mechanism of soil amplification is illustrated by Figure 6. The velocity observed at the bedrock surface shows only one half cycle of motion at significant amplitude and the velocity observed on the alluvium shows only two half cycles. The amplification of a broad-band signal such as this is obviously not primarily a resonance phenomena involving multiple reflections. Narrow-band measures such as the Fourier spectral amplitudes are, of course, affected by resonance but the amplification of the peak velocity shown in Figure 6 is simply the effect of the low shear-wave velocity in the near-surface materials and can be estimated by a relatively simple method from traditional seismological theory (Bullen, 1965), a method that does not require detailed information about site conditions. If we neglect losses due to reflection, scattering, and anelastic attenuation, the energy along a tube of rays is constant, and the amplitude is inversely proportional to the square root of the product of the density and the propagation velocity. If we include a correction for the change in cross-sectional area of the wave tube due to refraction in a medium where velocity is a function of depth we obtain an expression for the amplification ratio at a soil site

$$A = \left(\frac{\rho_R V_R}{\rho_R V_S}\right)^{1/2} \left(\frac{\cos i_R}{\cos i_S}\right)^{1/2}$$

where V_R and V_S are the near-surface velocities in rock and soil respectively, ρ_R and ρ_S are the densities and i_R and i_S are the angles of incidence. The factor involving the angles of incidence can be neglected in cases such as this where the angle of incidence in rock is not large. If the angle of incidence is neglected the expression reduces to one derived by Wiggins (1964) on a somewhat different basis. To use the expression one must decide over what interval the near-surface velocities should be measured. We propose a quarter wavelength down from the surface. In the case of stations numbers 1 and 2, estimating the dominant frequency for velocity at about 1 Hz, we obtain a value of 2.4 for the amplification ratio. This is somewhat smaller than the observed ratios for peak horizontal velocity (Table 1), as would be expected if some additional amplification mechanism such as focusing is operable; but it is reasonably close to the ratios computed for the linear model. Application of this approach to the amplification of peak acceleration requires modification to allow for the effect of anelastic attenuation in the alluvium. Estimating the dominant frequency for acceleration at 3 Hz we obtain an amplification ratio of 2.9, uncorrected for attenuation. Correcting for attenuation using a frequency of 3 Hz and the assumed Q of 16 gives a ratio of 2.3, which is similar to the observed values and also to the values computed for the linear model (Table 1). The effect of anelastic attenuation may account for the fact that at this site both peak horizontal acceleration and velocity show significant amplification on the alluvium whereas in the San Fernando earthquake (Boore et al., 1980) soil sites showed significant amplification in peak horizontal velocity but not acceleration. These relationships can be readily explained if, as would seem likely, there is a greater thickness of low-Q material on the average at the soil sites that recorded the San Fernando earthquake than at Gilroy station number 2.

ACKNOWLEDGEMENTS

We are indebted to Jerry P. Eaton for suggesting the Gilroy area as a location for the strong-motion array. Edward F. Roth made many contributions to this work beginning with installation of the instruments and their maintenance in the early years and ending with making arrangements for drilling at the instrument sites. We are also grateful to the personnel of the Seismic Engineering Branch of the U.S. Geological Survey, who have done the instrument maintenance in recent years. Darrell G. Herd assisted us with advice on the geology of the area. W. H. K. Lee kindly allowed us to use his aftershock map, and Ralph J. Archuleta, Paul Okubo, and Walter D. Mooney permitted us to cite unpublished conclusions of work in progress. Reviews by David M. Boore and Albert M. Rogers, Jr., lead to significant improvements in the manuscript.

REFERENCES

Andrews, D. J., and Shlien, S., 1972, Propagation of underground explosion waves in the nearly elastic range: Bull. Seism. Soc. Am. 62, p. 1691-1698.

Archuleta, R. J., 1979, Rupture propagation effects in the Coyote Lake earthquake (abstract): EOS, Trans. Am. Geophys. Union 60, p. 890.

Boore, D. M., Joyner, W. B., Oliver, A. A. III, and Page, R. A., 1978, Estimation of ground motion parameters: U.S. Geol. Survey Circular 795, 43 p.

Boore, D. M., Larner, K. L., and Aki, K., 1971, Comparison of two independent methods for the solution of wave-scattering problems: response of a sedimentary basin to vertically incident SH waves: J. Geophys. Res. 76, p. 558-569.

Borcherdt, R. D., 1970, Effects of local geology on ground motion near San Francisco Bay: Bull. Seism. Soc. Am. 60, p. 29-61.

Borcherdt, R. D., and Gibbs, J. F., 1976, Effects of local geologic conditions in the San Francisco Bay region on ground motions and the intensities of the 1906 earthquake: Bull. Seism. Soc. Am. 66, p. 467-500.

Brady, A. G., Mork, P. N., Perez, V., and Porter, L. D., 1980, Processed data from the Gilroy array and Coyote Creek records, Coyote Lake earthquake, 6 August 1979: U.S. Geol. Survey Open-File Report 81-42, 171 p.

Bullen, K. E., 1965, An Introduction to the Theory of Seismology: Cambridge University Press, 381 p.

Chen, A. T. F., and Joyner, W. B., 1974, Multi-linear analysis for ground motion studies of layered systems: Report No. USGS-GD-74-020, NTIS No. PB 232-704/AS, Clearinghouse, Springfield, VA 22151.

Constantopoulos, I. V., 1973, Amplification studies for a nonlinear hysteretic soil model: Research Report R73-46, Department of Civil Engineering, Massachusetts Institute of Technology, 204 p.

Dobry, R., Whitman, R. V., and Roesset, J. M., 1971, Soil properties and the one-dimensional theory of earthquake amplification: Research Report R71-18, Department of Civil Engineering, Massachusetts Institute of Technology, 347 p.

Faccioli, E., Santoyo V., E., and Leon T., J., 1973, Microzonation criteria and seismic response studies for the city of Managua: Proc. Earthquake Eng. Res. Inst. Conf. Managua, Nicaragua, Earthquake of Dec. 23, 1972, v. 1, p. 271-291.

Futterman, W. I., 1962, Dispersive body waves: J. Geophys. Res. 67, p. 5279-5291.

Haskell, N. A., 1953, The dispersion of surface waves on multilayered media: Bull. Seism. Soc. Am. 43, p. 17-34.

Haskell, N. A., 1960, Crustal reflection of plane SH waves: J. Geophys. Res. 65, p. 4147-4150.

Hays, W. W., Rogers, A. M., and King, K. W., 1979, Empirical data about local ground response: Proc. Second U.S. National Conf. Earthquake Eng., p. 223-232.

Herd, D. G., McLaughlin, R. J., Sarna-Wojcicki, A. M., Clark, M. M., Lee, W. H. K., Sharp, R. V., Sorg, D. H., Stuart, W. D., Harsh, P. W., and Mark, R. K., 1979, Surface faulting accompanying the August 6, 1979 Coyote Lake earthquake: EOS, Trans. Am. Geophys. Union 60, p. 890.

Hong, T.-L., and Helmberger, D. V., 1978, Glorified optics and wave propagation in nonplanar structure: Bull. Seism. Soc. Am. 68, p. 1313-1330.

Idriss, I. M., and Seed, H. B., 1968a, Seismic response of horizontal soil layers: Proc. Am. Soc. Civil Eng., J. Soil Mech. Found. Div. 94, SM4, p. 1003-1031.

Idriss, I. M., and Seed, H. B., 1968b, An analysis of ground motions during the 1957 San Francisco earthquake: Bull. Seism. Soc. Am. 58, p. 2013-2032.

Iwan, W. D., 1967, On a class of models for the yielding behavior of continuous and composite systems: J. Appl. Mech. 34, p. 612-617.

Joyner, W. B., and Chen, A. T. F., 1975, Calculation of nonlinear ground response in earthquakes: Bull. Seism. Soc. Am. 65, p. 1315-1336.

Joyner, W. B., Warrick, R. E., and Oliver, A. A., III, 1976, Analysis of seismograms from a downhole array in sediments near San Francisco Bay: Bull. Seism. Soc. Am. 66, p. 937-958.

Kanai, K., 1952, Relation between the nature of surface layer and the amplitudes of earthquake motions: Bull. Earthquake Res. Inst. Tokyo Univ. 30, p. 31-37.

Kanasewich, E. R., 1973, Time Sequence Analysis in Geophysics: University of Alberta Press, Edmonton, 352 p.

Lawson, A. C. (chairman), 1908, The California Earthquake of April 18, 1906, Report of the State Earthquake Investigation Commission: Carnegie Inst. Washington, Atlas maps 19, 21, and 22.

Lee, W. H. K., Herd, D. G., Cagnetti, V., Bakun, W. H., and Rapport, A., 1979, A preliminary study of the Coyote Lake earthquake of August 6, 1979 and its major aftershocks: U.S. Geol. Survey Open-File Report 79-1621, 43 p.

Matthiesen, R. B., Duke, C. M., Leeds, D. J., and Fraser, J. C., 1964, Site characteristics of southern California strong-motion earthquake stations, Part II: Report No. 64-15, Department of Engineering, University of California at Los Angeles.

Okubo, P. G., 1979, Spectral characteristics of the Coyote Lake earthquake and several of its aftershocks (abs.): Seism. Soc. Am., Earthquake Notes, 50, p. 63.

Porcella, R. L., Matthiesen, R. B., McJunkin, R. D., and Ragsdale, J. T., 1979, Compilation of strong-motion records from the August 6, 1979 Coyote Lake earthquake: U.S. Geol. Survey Open-File Report 79-385, 71 p.

Rogers, A. M., and Hays, W. W., 1979, Preliminary evaluation of site transfer functions developed from earthquakes and nuclear explosions: Proc. Second Inter. Conf. Microzonation (San Francisco, California), 2, p. 753-763.

Seed, H. B., and Idriss, I. M., 1970, Analysis of ground motions at Union Bay, Seattle, during earthquakes and distant nuclear blasts: Bull. Seism. Soc. Am. 60, p. 125-136.

Shima, E., 1962, Modifications of seismic waves in superficial soil layers as verified by comparative observations on and beneath the surface: Bull. Earthquake Res. Ins., Tokyo Univ. 40, p. 187-259.

Silva, W., 1976, Body waves in a layered anelastic solid: Bull. Seism. Soc. Am. 66, p. 1539-1554.

Streeter, V. L., Wylie, E. B., and Richart, F. E., Jr., 1974, Soil motion computations by characteristics method: Proc. Am. Soc. Civil Eng., J. Geotech. Eng. Div. 100, p. 247-263.

Tsai, N. C., and Housner, G. W., 1970, Calculation of surface motions of a layered half-space: Bull. Seism. Soc. Am. 60, p. 1625-1651.

Uhrhammer, R. A., 1980, Observations of the Coyote Lake, California earthquake sequence of August 6, 1979: Bull. Seism. Soc. Am. 70, p. 559-570.

Wiggins, J. H., Jr., 1964, Effect of site conditions on earthquake intensity: Proc. Am. Soc. Civil Eng., J. Structural Div. 90, ST2, p. 279-313.

Wood, H. O., 1908, Distribution of apparent intensity in San Francisco, in The California Earthquake of April 18, 1906, Report of the State Earthquake Investigation Commission, v. 1: Carnegie Inst., Washington, p. 220-245.

Table 1. Observed and predicted peak horizontal acceleration and velocity at Gilroy station numbers 1 and 2.

	Peak Transverse Acceleration	Peak Radial Acceleration	Peak Transverse Velocity	Peak Radial Velocity
Gilroy 1 observed*	0.10 g	0.11 g	8.9 cm/sec	5.5 cm/sec
Gilroy 2 observed*	0.24 g	0.26 g	28 cm/sec	20 cm/sec
predicted, linear model	0.17 g	0.23 g	15 cm/sec	12 cm/sec
predicted, nonlinear model, $\gamma = 1.0$	0.15 g		13 cm/sec	
predicted, nonlinear model, $\gamma = 0.5$	0.12 g		12 cm/sec	

*The peak values cited in the text apply to the components in the directions as originally recorded and are slightly different from the values for the radial and transverse components given here.

Figure 1. Map showing aftershocks for the first 15 days after the Coyote Lake earthquake (modified from Lee _et al._, 1979). Also shown are the strong motion stations (1, 2, 3, 4, 6) of the Gilroy array where records were obtained of the mainshock.

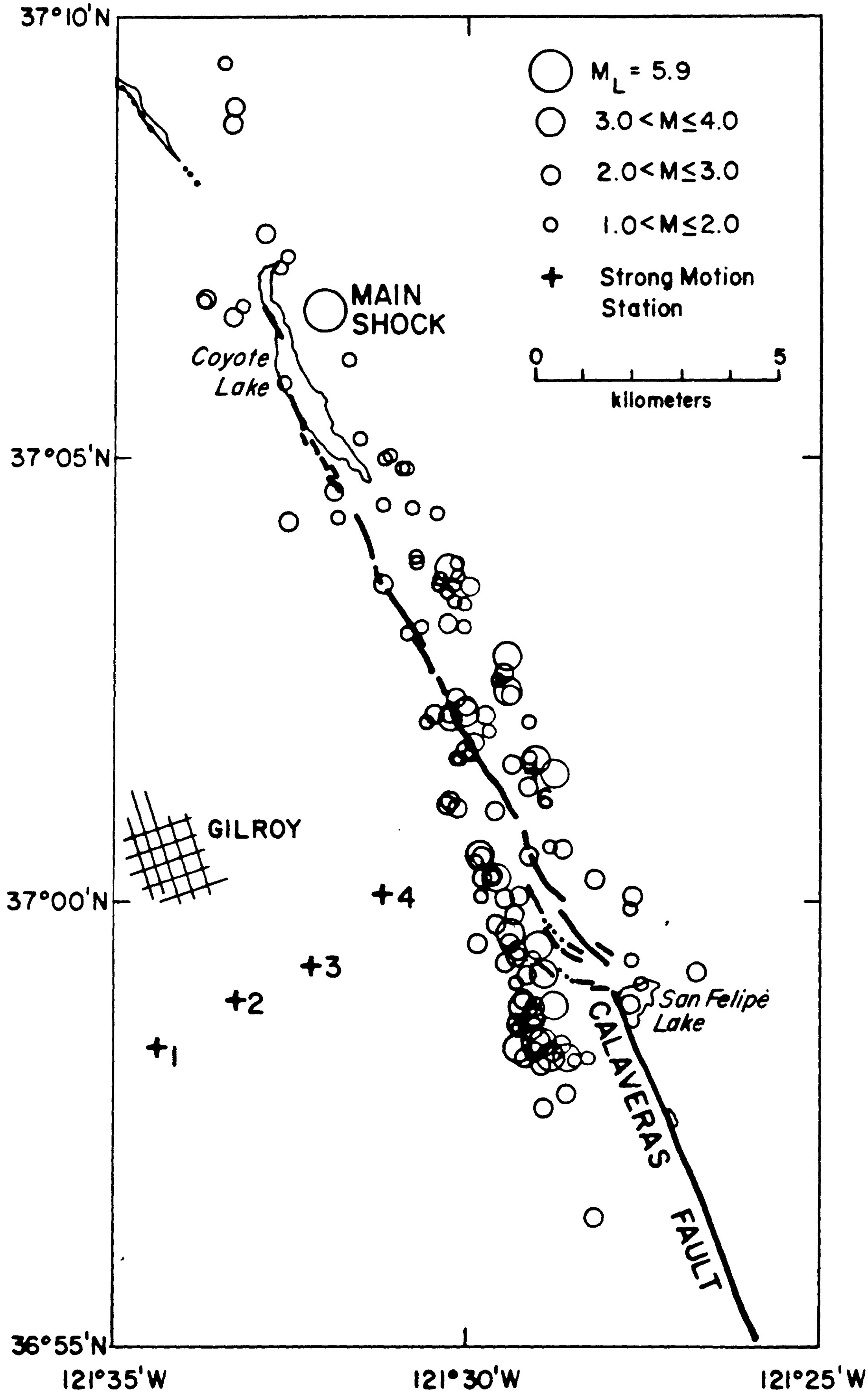

37°10'N
37°05'N
37°00'N
36°55'N
121°35'W
121°30'W
121°25'W
M_L = 5.9
3.0<M≤4.0
2.0<M≤3.0
1.0<M≤2.0
Strong Motion Station
0
5
kilometers
MAIN SHOCK
Coyote Lake
GILROY
+4
+3
+2
+1
San Felipe Lake
CALAVERAS FAULT

Fig. 1

Figure 2. Geologic log of the drill hole at the site of Gilroy station number 2.

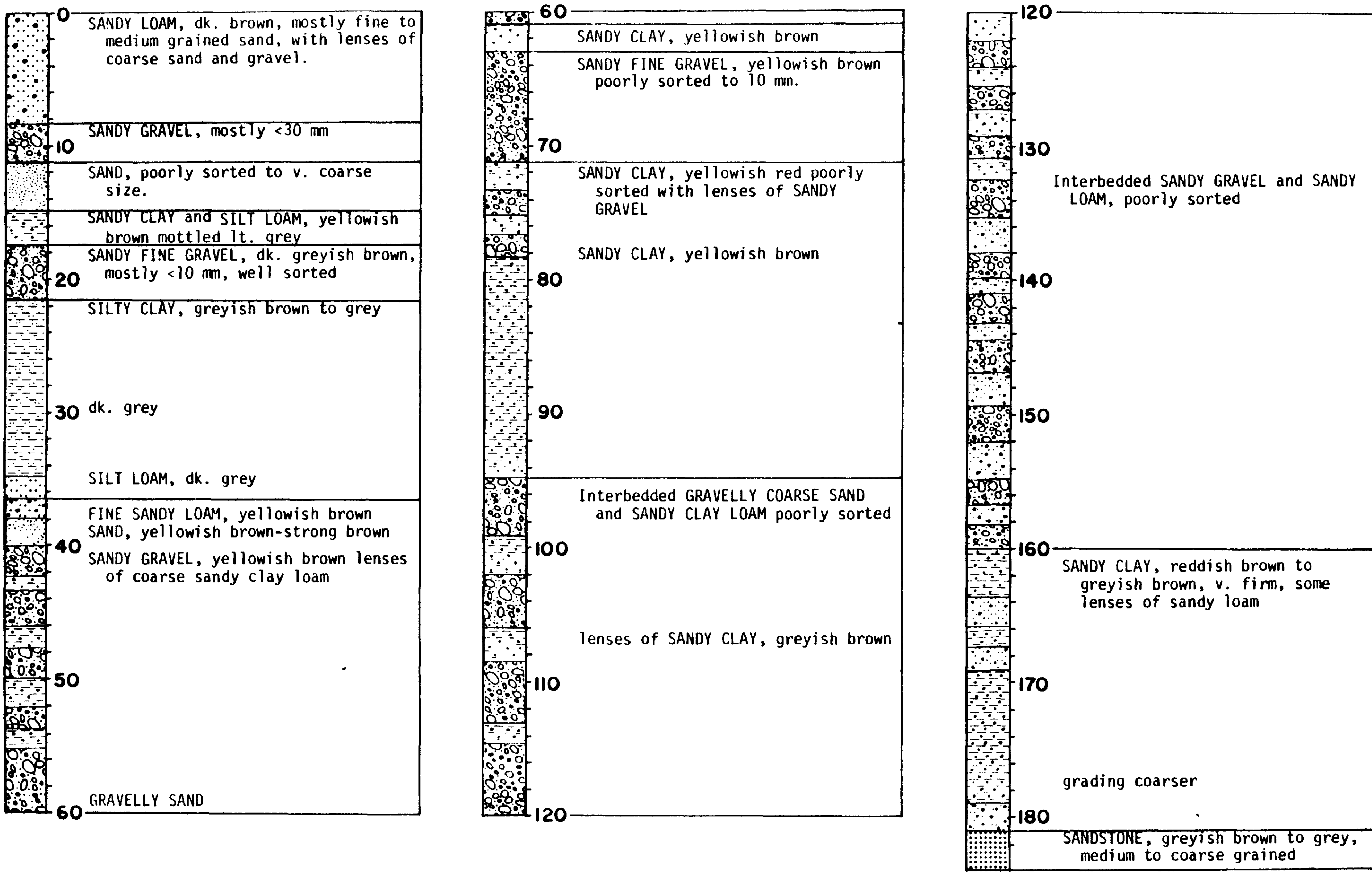
0
SANDY LOAM, dk. brown, mostly fine to medium grained sand, with lenses of coarse sand and gravel.
SANDY GRAVEL, mostly <30 mm
10
SAND, poorly sorted to v. coarse size.
SANDY CLAY and SILT LOAM, yellowish brown mottled lt. grey
SANDY FINE GRAVEL, dk. greyish brown, mostly <10 mm, well sorted
20
SILTY CLAY, greyish brown to grey
30
dk. grey
SILT LOAM, dk. grey
FINE SANDY LOAM, yellowish brown
SAND, yellowish brown-strong brown
40
SANDY GRAVEL, yellowish brown lenses of coarse sandy clay loam
50
GRAVELLY SAND
60
SANDY CLAY, yellowish brown
SANDY FINE GRAVEL, yellowish brown poorly sorted to 10 mm.
70
SANDY CLAY, yellowish red poorly sorted with lenses of SANDY GRAVEL
SANDY CLAY, yellowish brown
80
90
Interbedded GRAVELLY COARSE SAND and SANDY CLAY LOAM poorly sorted
100
lenses of SANDY CLAY, greyish brown
110
120
130
Interbedded SANDY GRAVEL and SANDY LOAM, poorly sorted
140
150
160
SANDY CLAY, reddish brown to greyish brown, v. firm, some lenses of sandy loam
170
grading coarser
180
SANDSTONE, greyish brown to grey, medium to coarse grained

Fig. 2

Figure 3. Velocity profiles for the site of Gilroy station number 2.

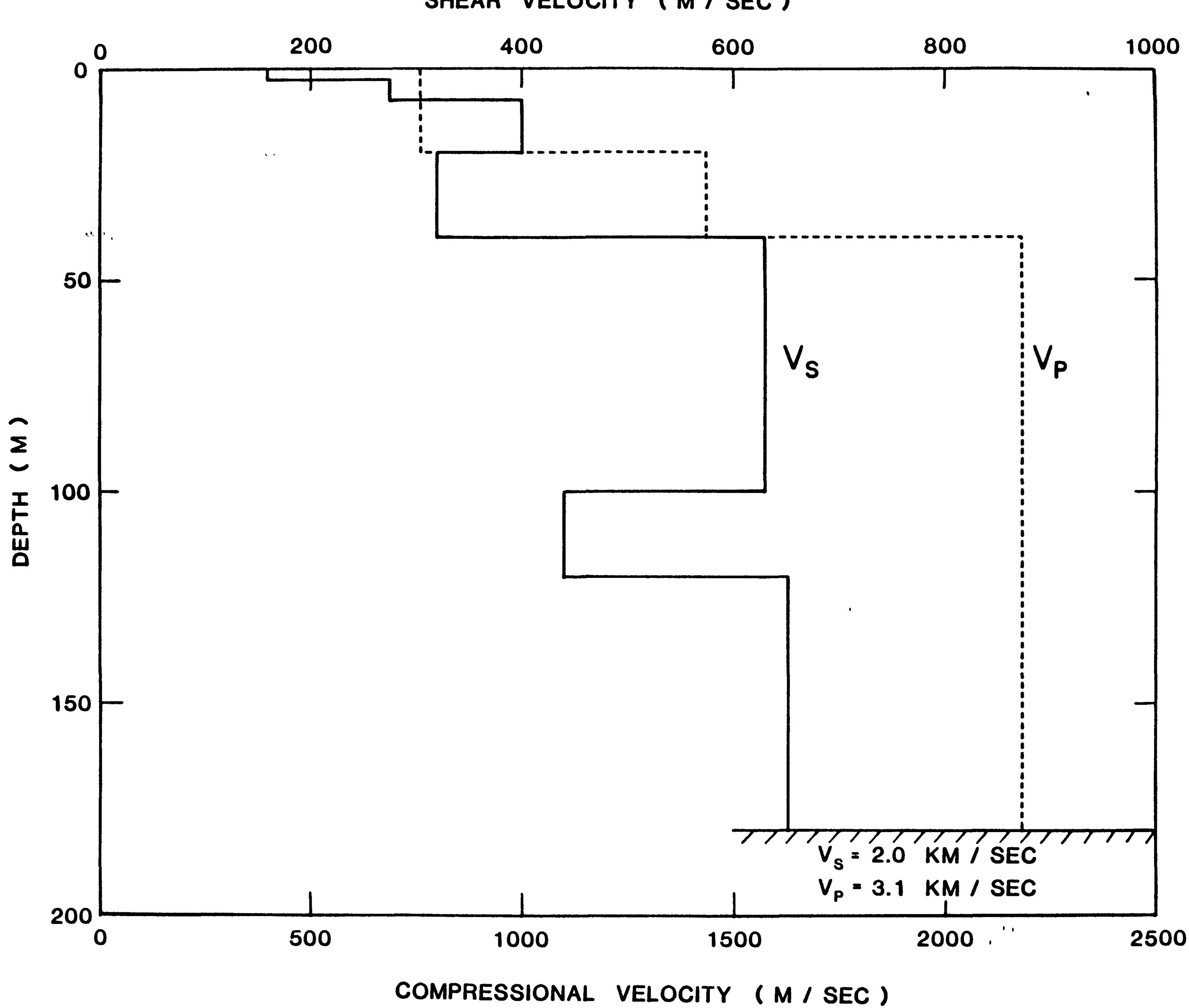
SHEAR VELOCITY (M / SEC)
0
200
400
600
800
1000
DEPTH (M)
0
50
100
150
200
V_S
V_P
V_S = 2.0 KM / SEC
V_P = 3.1 KM / SEC
0
500
1000
1500
2000
2500
COMPRESSIONAL VELOCITY (M / SEC)

Fig. 3

Figure 4. Transverse horizontal acceleration observed at Gilroy stations number 1 and 2 and calculated at station number 2 for the linear model.

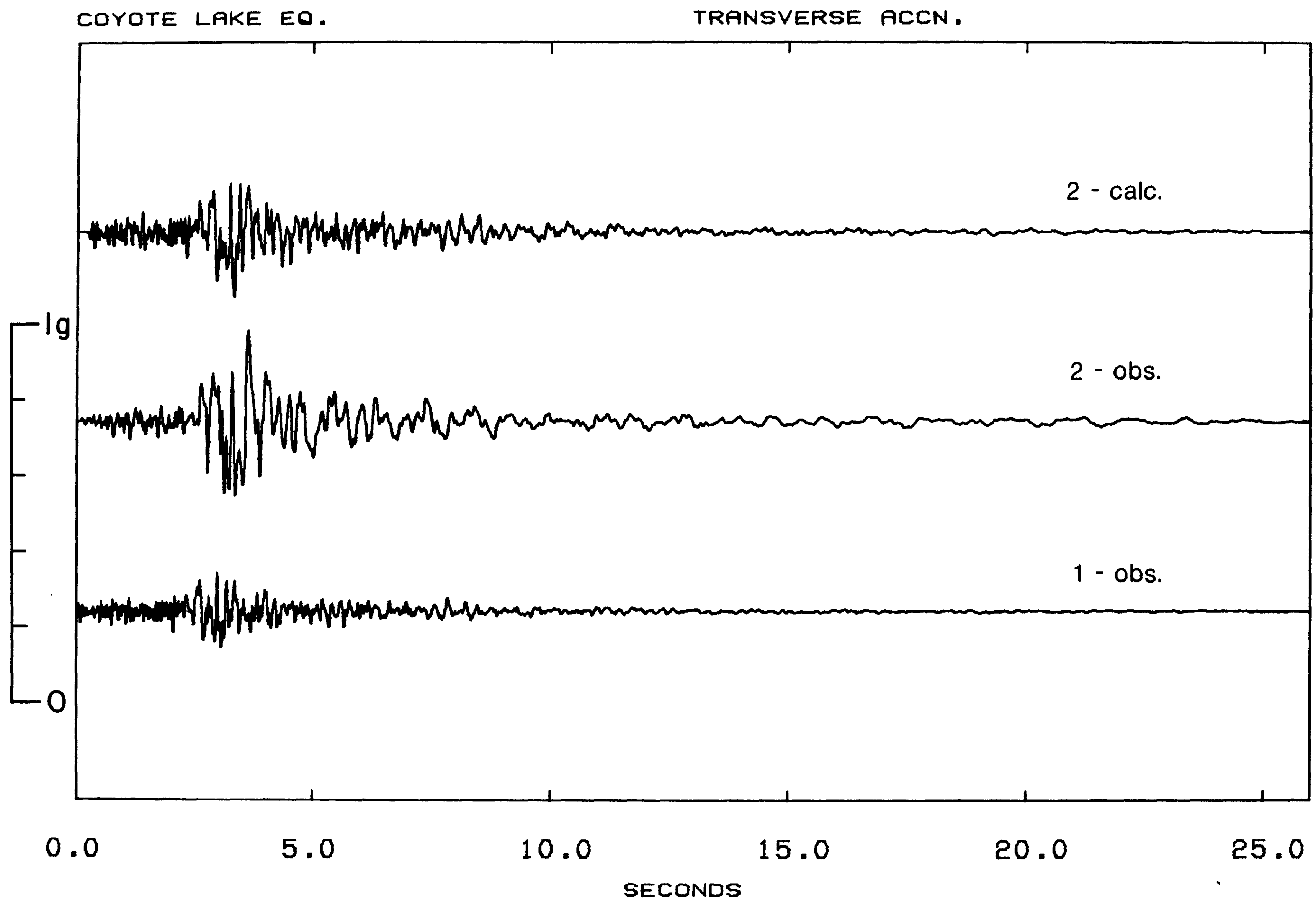

COYOTE LAKE EQ.
TRANSVERSE ACCN.
2 - calc.
2 - obs.
1 - obs.
1g
0
0.0
5.0
10.0
15.0
20.0
25.0
SECONDS

Fig. 4

Figure 5. Radial horizontal acceleration observed at Gilroy stations number 1 and 2 and calculated at station number 2 for the linear model.

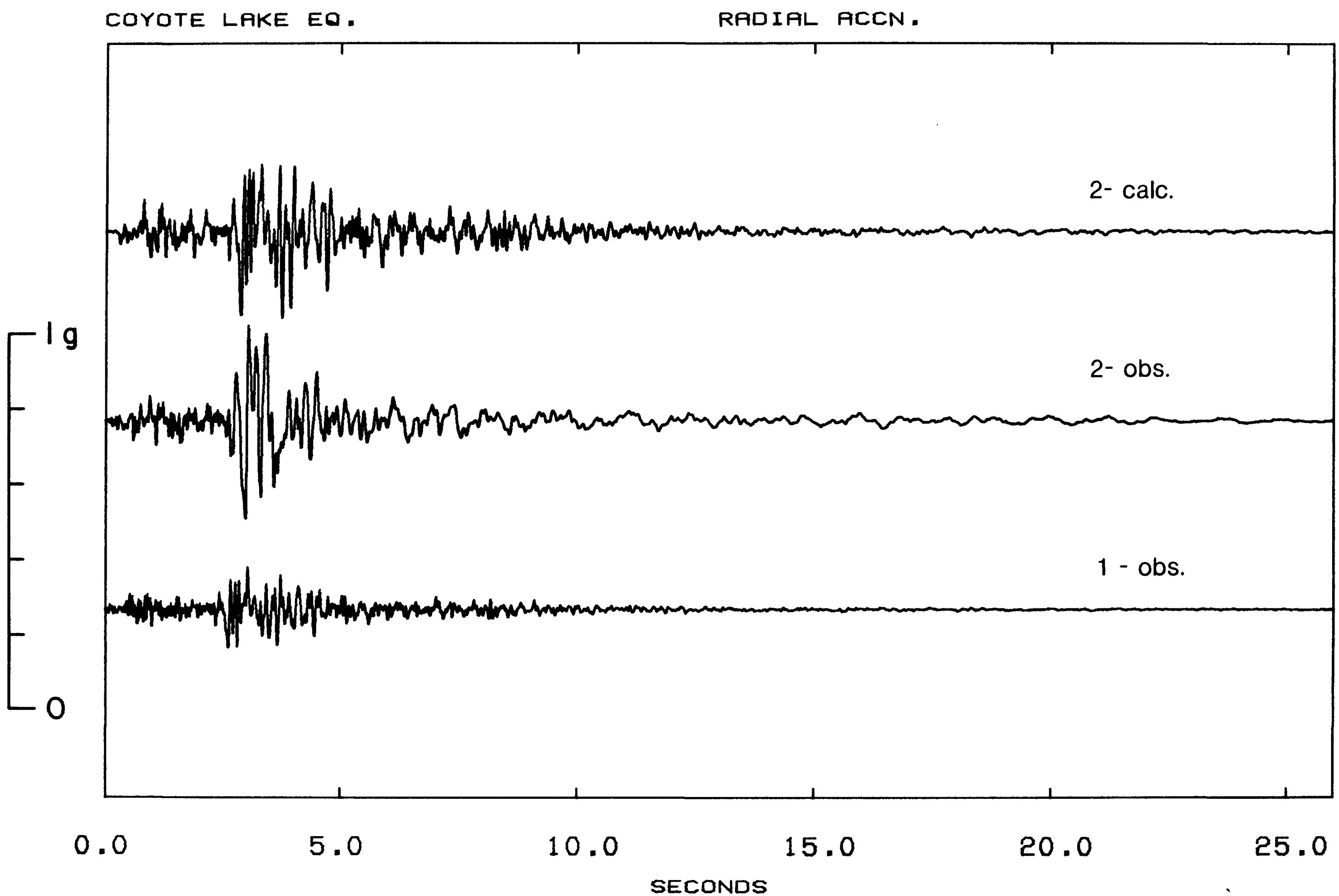
COYOTE LAKE EQ.
RADIAL ACCN.
2- calc.
2- obs.
1 - obs.
1g
0
0.0
5.0
10.0
15.0
20.0
25.0
SECONDS

Fig. 5

Figure 6. Transverse horizontal velocity observed at Gilroy stations number 1 and 2 and calculated at station number 2 for the linear model.

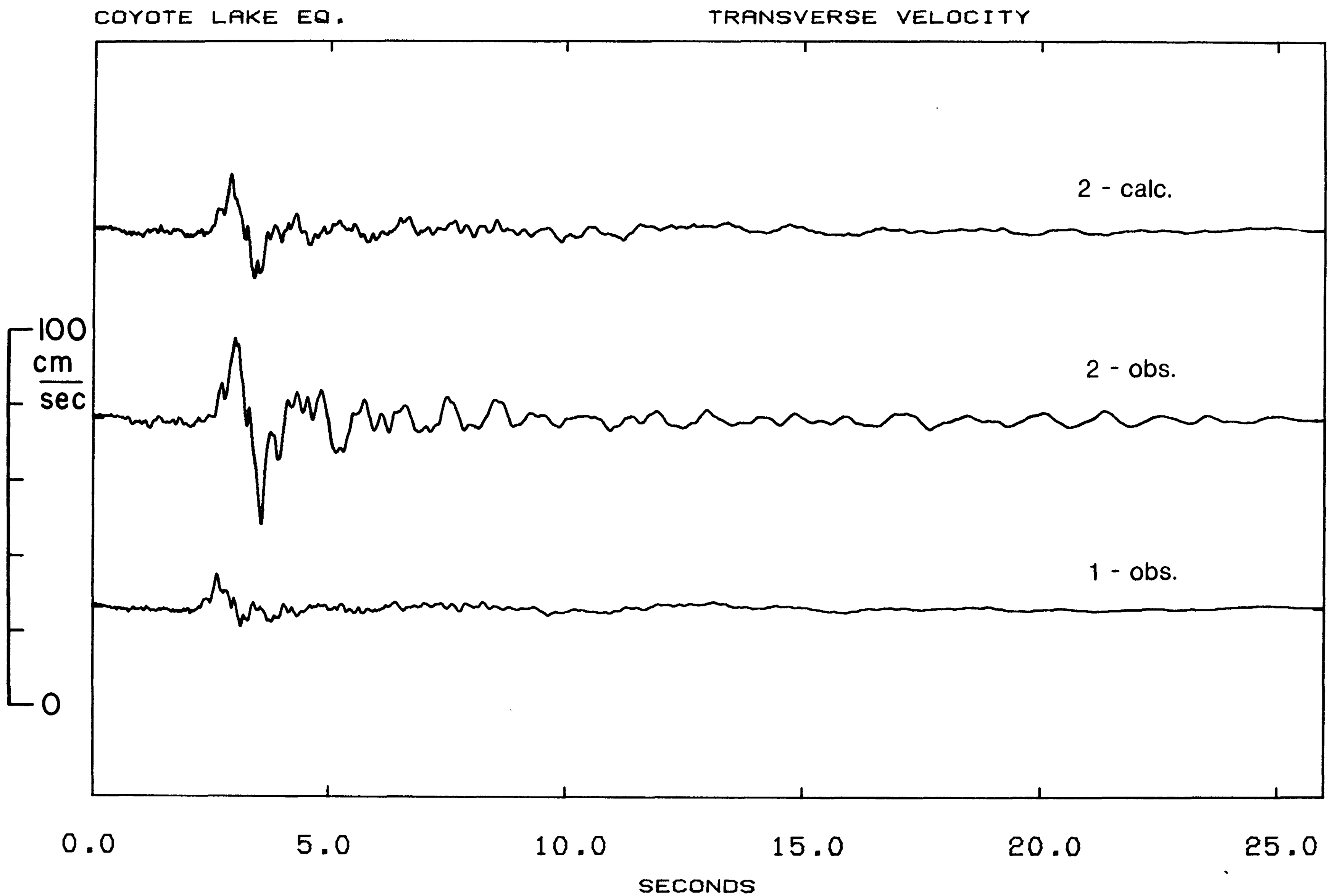

88575 01
BROOMALL INDUSTRIES INC

Fig. 6

Figure 7. Radial horizontal velocity observed at Gilroy stations number 1 and 2 and calculated at station number 2 for the linear model.

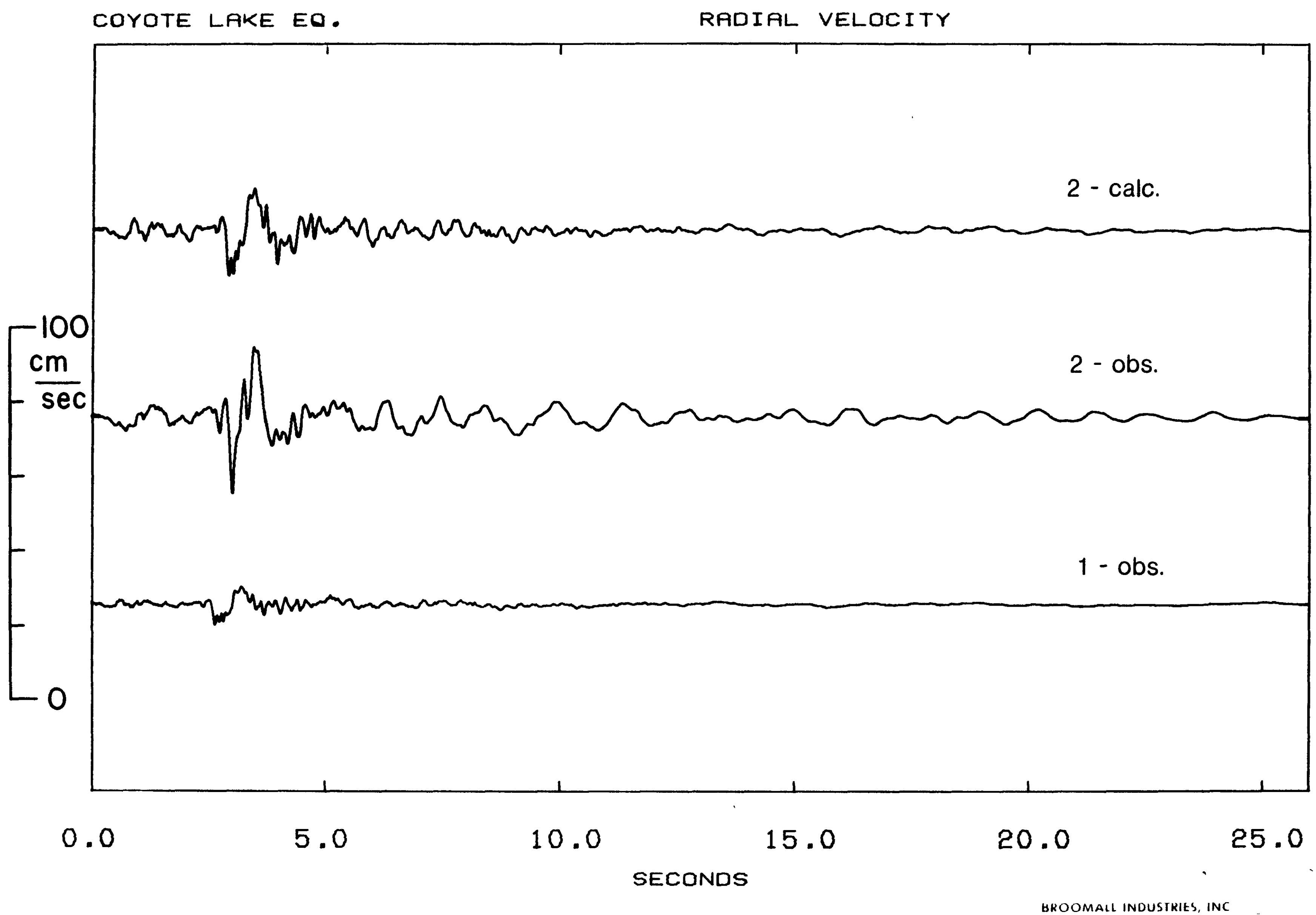
COYOTE LAKE EQ.
RADIAL VELOCITY
2 - calc.
2 - obs.
1 - obs.
100
cm
sec
0
0.0
5.0
10.0
15.0
20.0
25.0
SECONDS
BROOMALL INDUSTRIES, INC

Fig. 7

Figure 8. Spectral ratio of transverse (above) and radial (below) horizontal ground motion at Gilroy station number 2 relative to station number 1, observed and calculated for the linear model.

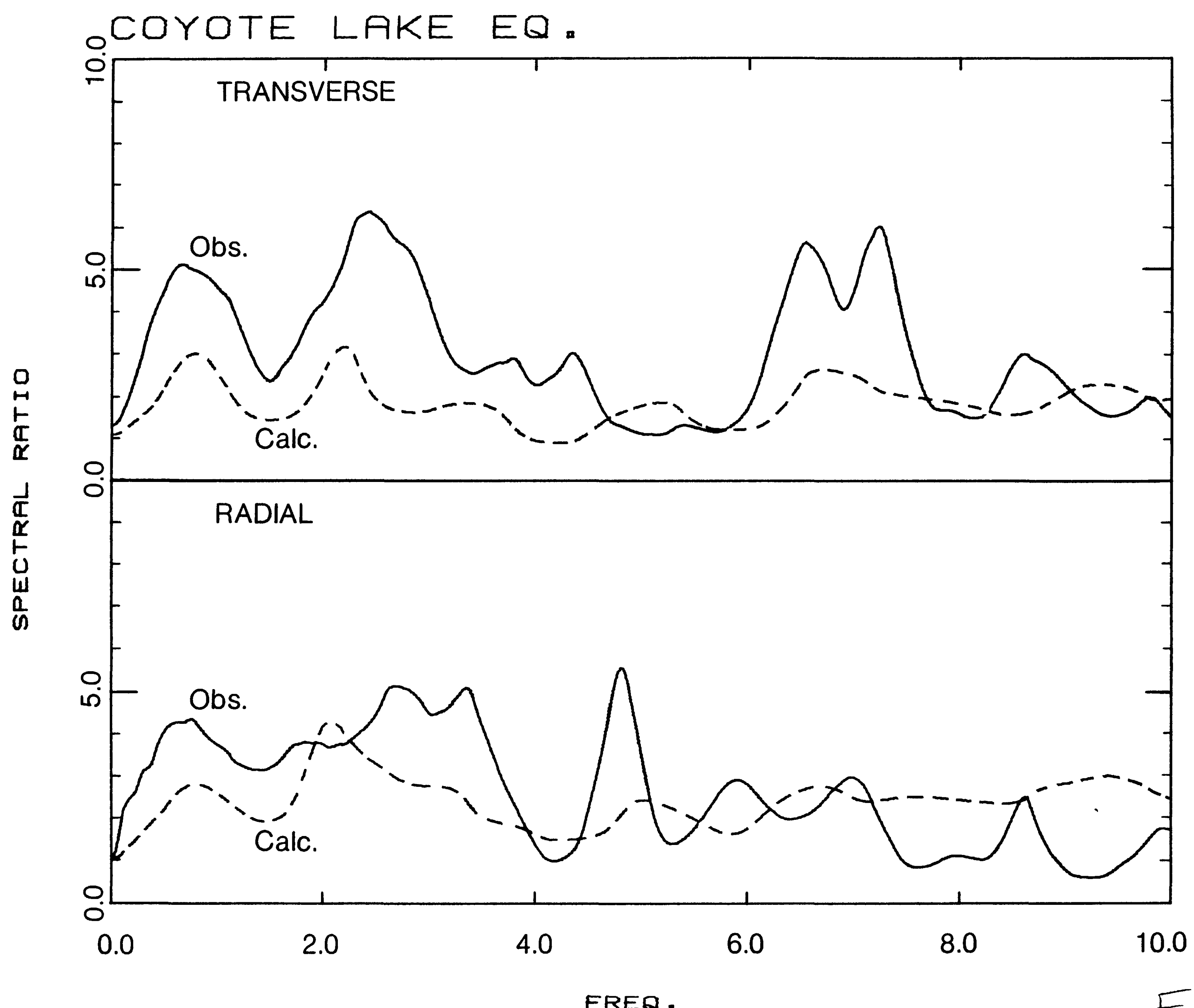
COYOTE LAKE EQ.
TRANSVERSE
RADIAL
Obs.
Calc.
Obs.
Calc.
SPECTRAL RATIO
FREQ.
0.0
5.0
10.0
0.0
5.0
0.0
0.0
2.0
4.0
6.0
8.0
10.0

Fig. 8

Figure 9. Model used for the nonlinear constitutive relationship.

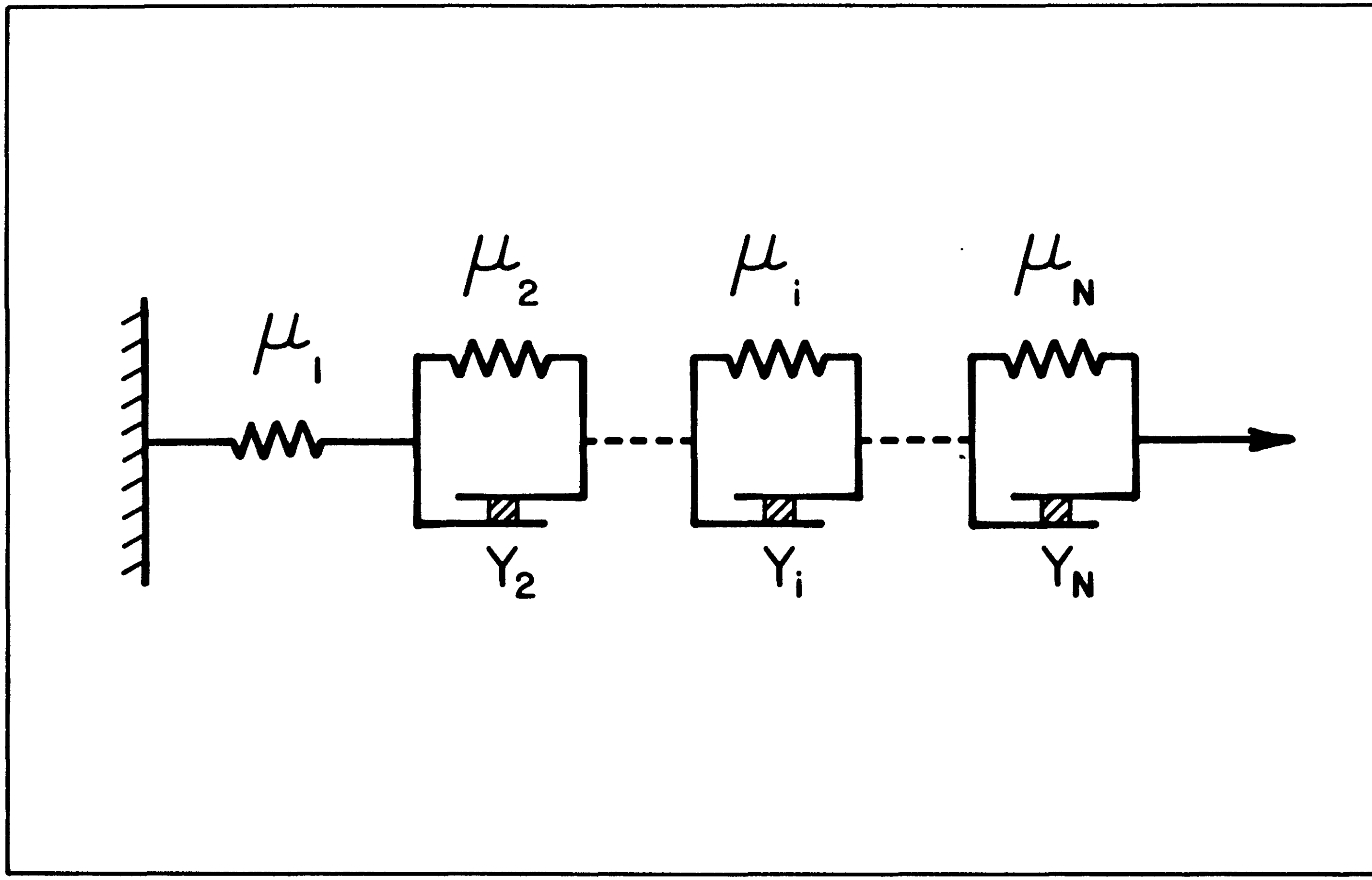

Fig. 9

Figure 10. Transverse horizontal acceleration observed at Gilroy stations number 1 and 2 and calculated at station number 2 for different models.

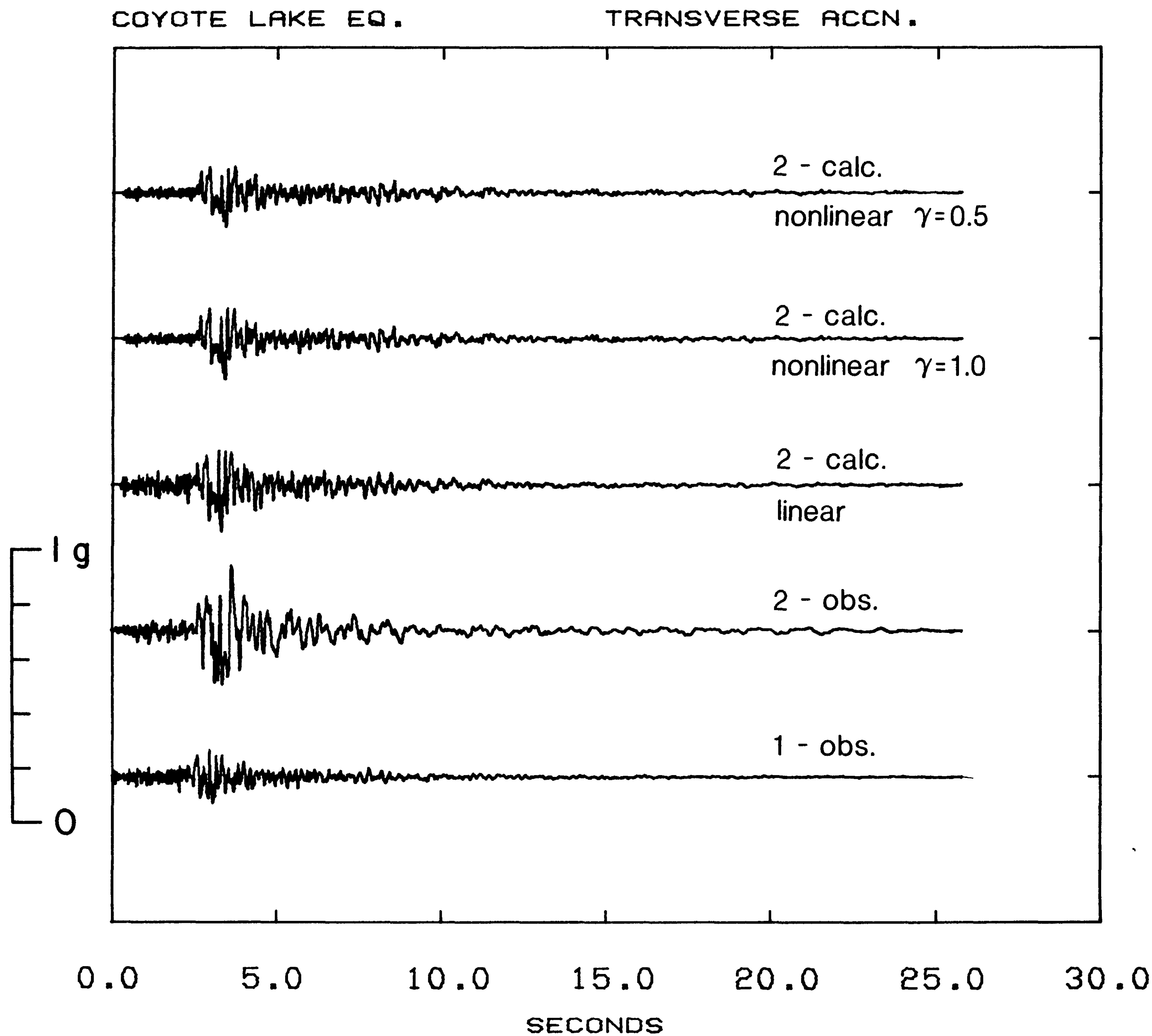
COYOTE LAKE EQ.
TRANSVERSE ACCN.
2 - calc.
nonlinear γ=0.5
2 - calc.
nonlinear γ=1.0
2 - calc.
linear
2 - obs.
1 - obs.
1 g
0
0.0
5.0
10.0
15.0
20.0
25.0
30.0
SECONDS

Fig. 10

Figure 11. Transverse horizontal velocity observed at Gilroy stations number 1 and 2 and calculated at station number 2 for different models.

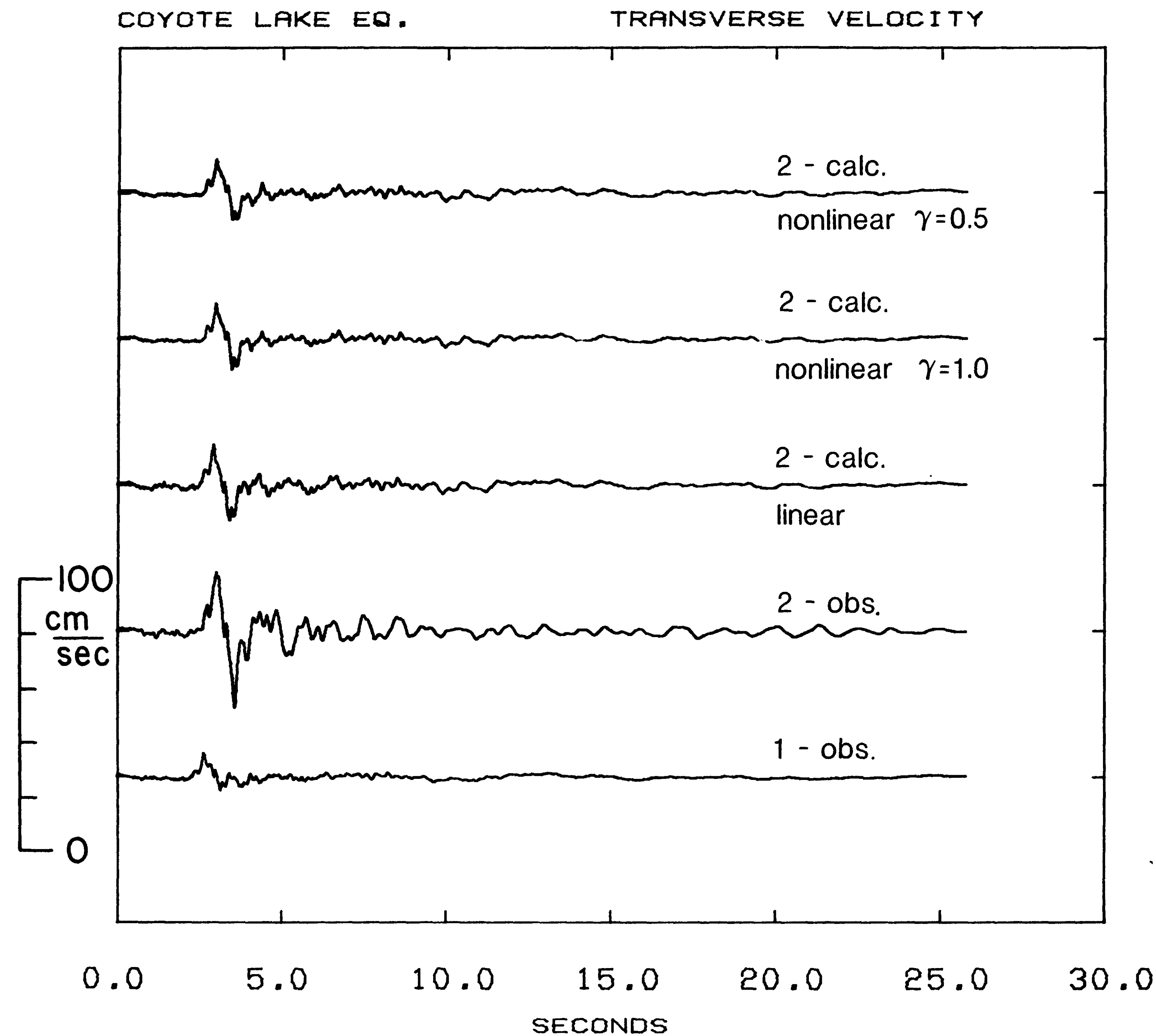
COYOTE LAKE EQ.
TRANSVERSE VELOCITY
2 - calc.
nonlinear γ=0.5
2 - calc.
nonlinear γ=1.0
2 - calc.
linear
2 - obs.
1 - obs.
100
cm/sec
0
0.0
5.0
10.0
15.0
20.0
25.0
30.0
SECONDS

Fig. 11